文章编号：1001-9014(2024)03-0354-05

DOI:10.11972/j.issn.1001-9014.2024.03.009

Non-destructive thickness measurement with micron level accuracy based on a 4.3-THz quantum-cascade laser

LI Hong-Yi[1,2], TAN Zhi-Yong[1,2*], WAN Wen-Jian[1,2], CAO Jun-Cheng[1,2*]

(1. National Key Laboratory of Materials for Integrated Circuits, Shanghai Institute of Microsystem and Information Technology, Chinese Academy of Sciences, Shanghai 200050, China;
2. Center of Materials Science and Optoelectronics Engineering, University of Chinese Academy of Sciences, Beijing 100049, China)

Abstract: A homodyne detection system to acquire the thickness of silicon wafers is constructed and described. By harnessing the relationship between the transmission phase change of a 4. 3-THz light beam and the incident angle controlled by a mechanical rotating stage, the thickness value of sample can be precisely deduced using the standard residual error method. The results indicate that the fitted thickness of the sample differs by only 2. 5~3 μm from more accurate results measured by optical microscopes, achieving terahertz non-destructive thickness measurement with micron level accuracy. The experiment validates the effectiveness of terahertz quantum-cascade laser in non-contact and nondestructive measurement.

Key words: terahertz, quantum-cascade laser, homodyne detection, non-destructive testing, non-contact measurement

基于4.3 THz量子级联激光器的微米级无损厚度测量

李弘义[1,2], 谭智勇[1,2*], 万文坚[1,2], 曹俊诚[1,2*]

(1. 中国科学院上海微系统与信息技术研究所,集成电路材料全国重点实验室,上海 200050;
2. 中国科学院大学材料科学与光电工程中心,北京 100049)

摘要:构建和描述了一种用于获取硅片厚度的零差检测系统。利用4.3-THz激光束的传输相变与机械旋转台控制的入射角之间的关系,可以使用标准残差法精确推导被测样品的厚度值。结果表明,样品的厚度拟合值与光学显微镜的精确测量结果仅相差2.5~3 μm,实现了微米级精度的太赫兹无损厚度测量。实验验证了太赫兹量子级联激光器在非接触无损测量中的有效性。

关 键 词:太赫兹;量子级联激光器;零差探测;无损检测;非接触测量

中图分类号:TN219　　**文献标识码**:A

Introduction

Terahertz light with a good transparency in most dielectrics can penetrate a certain thickness of material and achieve high-precision imaging. It thus can promise a wide range of applications in non-destructive testing and non-contact measurement [1]. Compared to the direct detection scheme, laser coherent detection has the advantages of acquiring multiple information features with high sensitivity, and is widely used in high-precision detection [2]. For example, it can detect the phase information of light, which can help reveal more properties of the materials, such as refractive index, thickness, and stress. In various coherence detection techniques, the homodyne detection [2] is widely used for the detection of material stress and thickness in the visible and infrared bands [3, 4] due to its simplicity and effectiveness. In the meanwhile, Terahertz quantum cascade laser (QCL) [5] is a promising compact laser source in 1 to 5 THz range, and has good applications in local oscillation source [6], multi-color imaging [7], real-time imaging [8], near-field imaging [9], etc. The light emitting from the terahertz QCLs has high monochromaticity and coherence proper-

Received date:2023-08-28, **revised date**:2023-09-10　　**收稿日期**:2023-08-28,**修回日期**:2023-09-10

Foundation items:Supported by National Natural Science Foundation of China (61927813, 62035014, 62275258), and Science and Technology Commission of Shanghai Municipal (21ZR1474600).

Biography:Li Hongyi (1996-), male, Hebei, Doctor. Research area involves terahertz detection and optoelectronic testing. Email: hyli@mail.sim.ac.cn

*Corresponding author:Email: zytan@mail.sim.ac.cn, jccao@mail.sim.ac.cn

ties [10], which is suitable for homodyne detection.

In this letter, a homodyne detection system at a working frequency of 4.3 THz is built by employing a terahertz QCL and a terahertz array detector. Two terahertz beam splitters and two gold coated mirrors are used to construct a terahertz coherent optical path, and a terahertz lens is utilized to form the interference fringes which are detected and clearly displayed by a terahertz array detector. By introducing a precision rotating mechanism into one branch of the optical path, the transmission phase curve used to fit the thickness of the measured sample is acquired. Finally, based on the standard residual error fitting method, the thickness fittings of multiple high-resistivity silicon wafers are realized. The fitting results are compared with the higher precision measurement results from optical microscopes, from which the accuracy of the above thickness measurements is roughly estimated.

1 Experiments

The schematic diagram and photos of the terahertz homodyne detection system are shown in Fig. 1 (a) and (b), respectively. The emitted light from the terahertz QCL is a collimated beam with a diameter of about 3 mm. B1 and B2 are two high-resistivity silicon beam splitters with a diameter of 3 inches and a thickness of 1 mm, while M1 and M2 are gold-coated planar mirrors with a diameter of 2 inches. B1, M1, and M2 are all placed vertically at a strict 45° or -45° to the direction of light propagation. L1 is a high-resistivity silicon lens, where the local oscillator light passing through B2 converges with the signal light reflected by B2 and reaches the terahertz detector. In order to observe the changes in interference fringes on the terahertz array detector, the angle between B2 and the direction of light propagation is slightly less than 45°.

The terahertz QCL, operating at 77 K, is placed in a liquid nitrogen dewar and has the same active region and fabrication process as Ref. 11. The size of the laser is 100 μm × 2 mm. The working center frequency and the average output power of the laser are about 4.3 THz and 0.8 mW, respectively. The terahertz array used in this experiment is a commercial detector which has an array size of 320 × 240. The pixel size of the array is 23.5 μm. The noise equivalent power (*NEP*) is about 100 pW/Hz$^{1/2}$ [12].

After the parallel light beam from QCL passes through the beam splitter B1, it is divided into two branches of reference beam and object beam. The former will enter the array along a straight line, and meet the latter which is directed by two mirrors M1 and M2 to go through the sample. In the experiments, for a high accuracy of the calculation, these three components of B1, M1, and M2 should be strictly aligned at an angle of 45° with respect to the incident beam. B2 is not strictly 45° for exhibiting the interference fringes. Specifically, the object light has a certain phase distribution on the array plane, allowing the interference fringes to be distinguishable at the detector array.

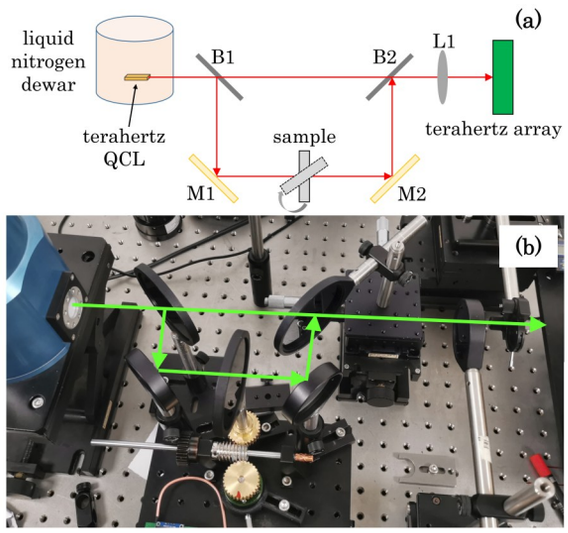

Fig. 1 Terahertz homodyne detection system: (a) Schematic of the terahertz light path; (b) Photos of the experimental setup
图1 太赫兹零差探测系统. (a) 太赫兹光路示意图; (b) 实验装置照片

2 Results and discussions

Firstly, in order to verify the coherence property of the terahertz beam used, a terahertz detector array was used to measure the terahertz interference fringes at the convergence point after L1 without the sample between M1 and M2. The measurement result is shown in Fig. 2.

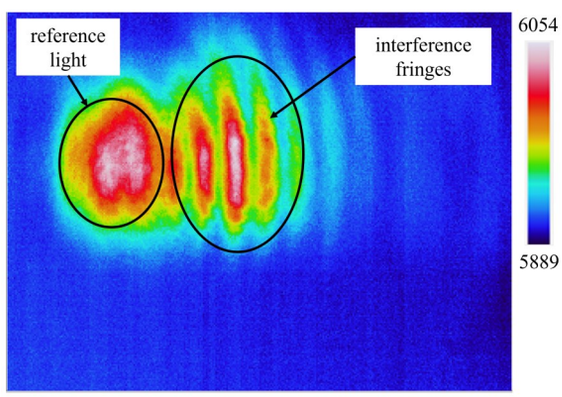

Fig. 2 The measured terahertz beam spot including both the reference light and the interference fringes
图2 测量得到的包括参考光和干涉条纹的太赫兹束斑

From Fig. 2, it can be seen that the interference fringes formed by the signal light and the reference light are very clear, with similar intervals between the interference fringes, indicating that the light emitted from the terahertz QCL has good coherence property. In Fig. 1, as M1 and M2 move downwards as a whole part, the interference fringes presented in Fig. 2 will shift, which corresponds to the phase change of the two coherent beams of light on the sensitive area of the terahertz array. By utilizing the above changes, we can obtain the optical path difference formed by M1 and M2 moving as a whole

part and its relationship with the light wavelength.

The above phase change can also be achieved by placing a transparent sample between M1 and M2, with the thickness changing. It should be noted that the sample must be a substance that can be easily penetrated by the terahertz light. In order to quickly achieve the change in sample thickness, we loaded the sample onto a rotational mechanical stage. The rotation of the sample leads to a change of terahertz light pathway inside the sample, resulting in changes in the optical path and the phase difference at the interference fringes.

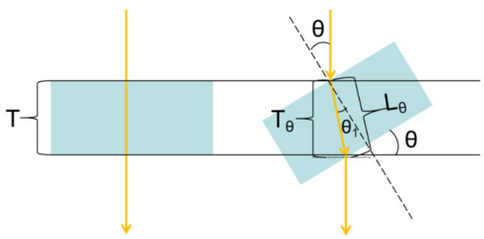

Fig. 3 Schematic diagram of the optical path when the terahertz beam passes through the sample
图3 太赫兹光束通过样品时的光路传播示意图

By utilizing the coherence property of the light emitted from terahertz QCL, we can deduce the thickness (T) of solid samples with parallel front and rear surfaces using the aforementioned homodyne detection system. Fig. 3 shows a schematic diagram of the optical path in the sample to be tested under two different incidence angles of terahertz light. According to the law of refraction, we can obtain that when the incidence angle is θ, the actual travel distance of terahertz light in the tested sample is determined by equation (1), while the distance projected from this distance to the direction of incident light satisfies equation (2).

$$L_\theta = \frac{T}{\cos\theta_1}, \quad (1)$$

$$T_\theta = L_\theta \cos(\theta - \theta_1), \quad (2)$$

When the sample is rotated, the accumulated phase through the sample at the incident light with the wavelength λ will be changed by a difference of transmission phase (φ) given by equation (3) with respect to that at normal incidence. It should be noted that, the rotation angle of the sample is equal to the incident angle (θ).

$$\varphi = 2\pi \times \left(\frac{n^2 T}{\lambda \sqrt{n^2 - \sin^2\theta}} + \frac{T\left(1 - \cos\theta - \frac{\sin^2\theta}{\sqrt{n^2 - \sin^2\theta}}\right)}{\lambda} - \frac{nT}{\lambda} \right), \quad (3)$$

As shown in Fig. 4, using equation (3), the curves between the rotation angle and the transmission phase of high-resistivity silicon wafers, with a typical refractive index value of 3.4, were calculated under different thicknesses T. It should be noted that when the sample is too thin, during the sample rotating, its phase transformation finally becomes too flat, resulting in the inability to achieve a period transformation exceeding 2π. Therefore, without changing the phase detection method, this method cannot directly measure very thin samples, and it needs to be modified by increasing the number of samples, that is, increasing the total thickness of the sample.

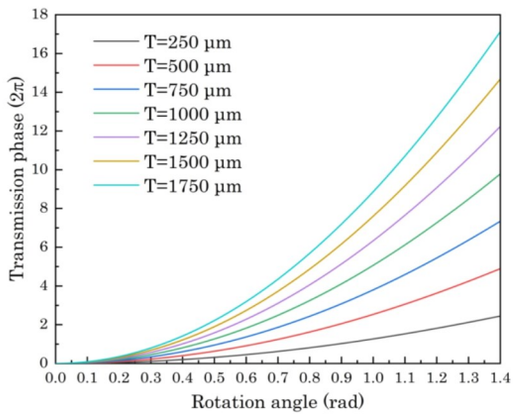

Fig. 4 Theoretical curves of transmission phase (φ) changing with sample rotation angle (θ) under different thickness (T) conditions
图4 不同厚度(T)条件下,传输相位(φ)随转角(θ)变化的理论计算值

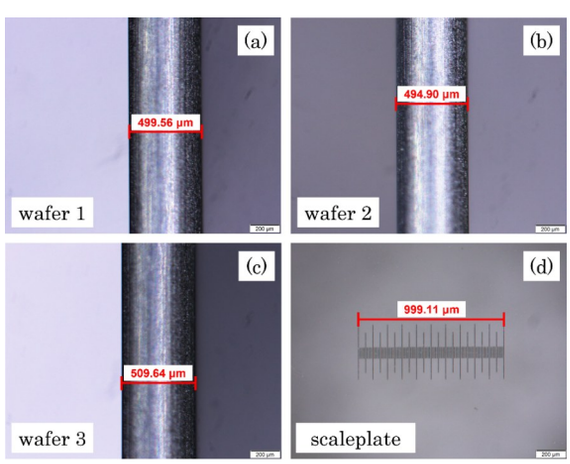

Fig. 5 Thickness measurement results of silicon wafers numbered 1 (a), 2 (b), and 3 (c) based on optical microscopes, as well as the measured length of a 1 mm standard microscale plate (d)
图5 基于光学显微镜的硅片厚度测量结果:(a)晶圆编号1;(b)晶圆编号2;(c)晶圆编号3,以及(d)1mm标准微刻度尺的长度测量结果

In this letter, we selected three 4-inch silicon wafers with a nominal thickness of 500 μm ± 10 μm for thickness measurement verification. Firstly, we accurately measured the thickness of the silicon wafer using an optical microscope (Olympus SZX16 with DP27 camera), and the measurement results are shown in Fig. 5. The silicon wafers are numbered 1, 2, and 3, with corresponding measured thicknesses of 499.56 μm, 494.90 μm, and 509.64 μm, respectively. Based on the actual

measured length of the one-millimeter micro-scale plate, the actual thickness of the silicon wafers numbered 1, 2, and 3 was calibrated to be 500.00 μm, 495.34 μm, and 510.09 μm, respectively. The thickness measurement accuracy of the above microscope is at the sub-micron level. Then, we divided three silicon wafers into two groups, one group composed of a combination of wafer 1 and wafer 2, and the other group composed of a combination of all three silicon wafers. Finally, we used the aforementioned terahertz homodyne detection scheme to measure the thickness of two sets of silicon wafers.

During the measurement, we loaded the silicon wafers on a rotating mechanical stage via a circular holder and aligned the center of the wafers with the rotation axis to ensure that the terahertz beam passes through the center of the silicon wafers. As shown in Fig. 2, we placed a terahertz detector array near the converging point shown in Fig. 1, and observed the interference fringes of terahertz light. When the rotating stage drives the sample to be inclined with respect to the incident beam, the phase of terahertz light passing through the silicon wafers undergoes continuous changes, and the interference fringes observed on the detection array shift. We can obtain the numerical relationship between the rotation angle of the silicon wafers and the transmission phase by determining the number of movements of the interference fringes and synchronously recording the rotation angle of the silicon wafers. For example, when the fringes on both sides move to the same position, it is considered that the transmission phase has changed by 2π. The relationship between the transmission phase and rotation angle of two sets of samples, wafer (1+2) and wafer (1+2+3), is shown in Fig. 6.

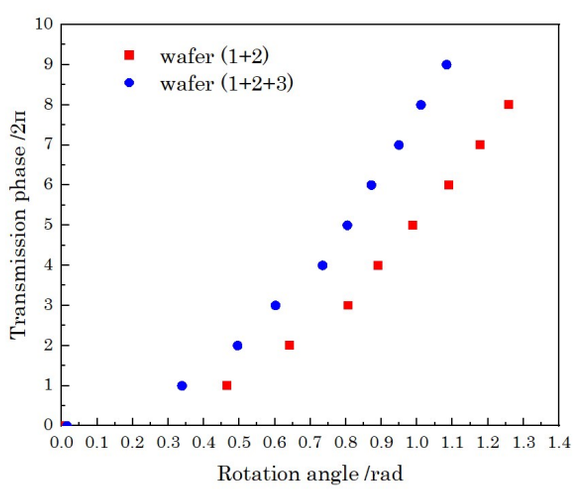

Fig. 6 Experimental results of transmission phase (φ) with the rotation angle (θ) after the terahertz light passes through the wafer (1+2) and the wafer (1+2+3)
图6 THz光透过晶圆(1+2)和晶圆(1+2+3)后传输相位(φ)随样品旋转角(θ)变化的实验测量结果

Fig. 7 shows the curve of RMSE with the fitting thickness during the fitting process of the transmission phase curve for the two groups of silicon wafer combinations. As shown in the figure, when the tested samples are two and three silicon wafers, the minimum RMSE values for fitting the transmission phase curve are 0.109 and 0.107, respectively. The fitting thickness values are 992.50 μm and 1503.00 μm, respectively. The corresponding fitting curve of the transmission phase and fitting values of thickness can be obtained, as shown in Fig. 8 and Tab. 1, respectively.

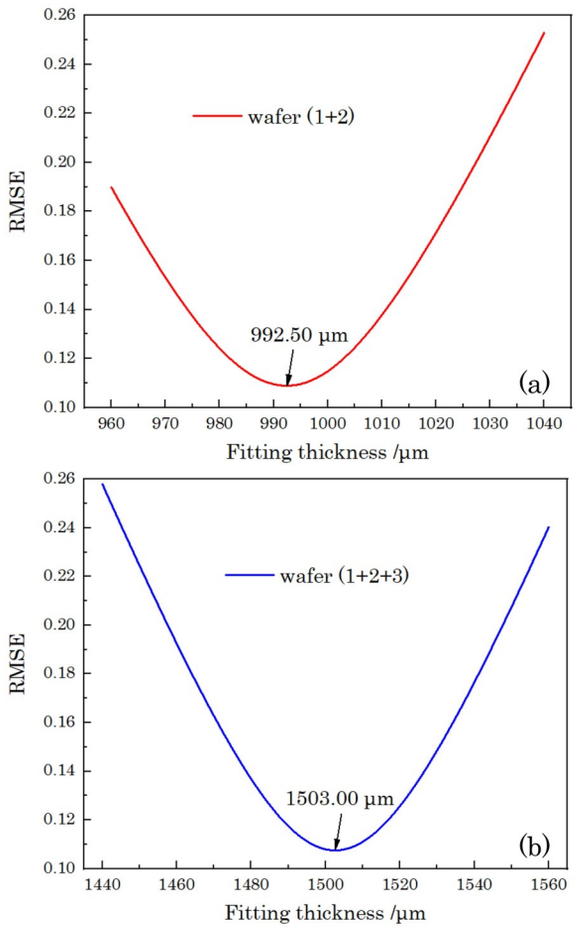

Fig. 7 Variation of the calculated RMSE with the fitting thickness: (a) wafer (1+2); (b) wafer (1+2+3)
图7 RMSE计算值随拟合厚度的变化:(a) 晶圆(1+2);(b) 晶圆(1+2+3)

Due to the fact that with the above method of observing the movement of interference fringes, one cannot directly obtain the thickness of the tested sample, we need to use a suitable method to fit the phase change curve to indirectly obtain the thickness of the tested samples. For this reason, for the curve fitting process in this letter we adopted the standard residual error fitting method. That is, for a given set of (T_0, n_0), we can obtain the residual error of the transmission phase as follows,

$$e_i = \varphi_i - \hat{\varphi}_i = \varphi_i - f(\theta_i, T_0, n_0) \quad , \quad (4)$$

where i=1, 2, ⋯, m. By calculating the root mean square error (RMSE), it is possible to determine whether the curve fitting is good or not. Through m iterations (i =m), the minimum RMSE is obtained, resulting in (T_m, n_m). We used a value of 3.4 for both n_0 and n_m as the re-

fractive index of silicon.

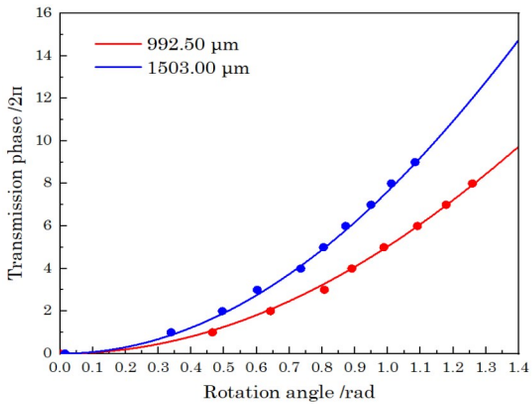

Fig. 8 Experimental (solid circle) and fitting (solid line) transmission phase with different rotation angle
图8 传输相位随不同旋转角度变化的实验测量(实心圆)和理论拟合(实线)结果

From Table 1, it can be seen that compared with the results measured by the optical microscope, the results obtained by the terahertz homodyne detection technique are very close. The measured thickness differences are about 3 μm and 2.5 μm, respectively. Although there is a little difference between the two methods, the method used in this letter can measure the thickness of any position on the silicon wafer as needed, and thus has better applicability compared to the fact that optical microscopes can only sample or measure the edges of the silicon wafer. In this means, the non-destructive property of THz technique is fully revealed.

Table 1 The nominal value and measurement results of the thicknes of different silicon wafers
表1 不同硅片的厚度标称值与测量结果

Wafer number	Nominal thickness (μm)	Thickness with an optical microscope (μm)	Thickness with homodyne detection (μm)
1	500 ± 10	500.00	/
2	500 ± 10	495.34	/
3	500 ± 10	510.09	/
1, 2	1 000 ± 20	995.43	992.50
1, 2, 3	1 500 ± 30	1 505.52	1 503.00

The above thickness measurement method is based on the correspondence between the number of movements (i.e., the transmission phase change is an integer multiple of 2π) of the interference fringes and the rotation angle of the sample, and there is a certain error in determining the movement of the interference fringes. In order to obtain more accurate results, a fast detector, such as a terahertz quantum-well photodetector [13-15], can be used to directly measure the intensity of interference light at specific interference fringes. In that case the change in transmission phase is obtained as an integer multiple of π or π/2, corresponding to a more precision sample rotation angle.

3 Conclusions

In summary, we have constructed a homodyne detection system using the terahertz quantum-cascade laser as the coherent light source and the terahertz array as the coherent beam detector. By employing a precise rotating stage to drive the measured samples to rotate, periodic variation of the transmission phase was obtained. By recording this periodic variation and combining it with the standard residual error fitting method, non-destructive thickness measurements of high-resistivity silicon wafers were achieved. For nominal thicknesses with 1 500 ± 30 μm and 1 000 ± 20 μm, the measurement results are 1 503.00 μm and 992.40 μm, respectively. The results exhibit very good agreement with those from the optical microscope, with a difference of about 2.5 μm and 3.0 μm, respectively. The above micron level non-destructive thickness measurement method based on terahertz homodyne detection system has the characteristics of non-contact and non-destructive testing and can measure any position of the sample, providing an effective method for high-precision thickness measurement in terahertz applications.

References

[1] Tonouchi M. Cutting-edge terahertz technology [J]. *Nature Photonics*, 2007, **1**: 97-105.
[2] Barry J R, Lee E A. Performance of coherent optical receivers [J]. *Proceedings of the IEEE*, 1990, **78**(8): 1369-1394.
[3] Baldi A. Residual Stress Analysis of Orthotropic Materials Using Integrated Digital Image Correlation [J]. *Experimental Mechanics*, 2014, **54**(7): 1279-1292.
[4] Disawal R, Suzuki T, Prakash S. Simultaneous measurement of thickness and refractive index using phase shifted Coherent Gradient Sensor [J]. *Optics and Laser Technology*, 2016, **86**: 85-92.
[5] Köhler R, Tredicucci A, Beltram F, *et al*. Terahertz semiconductor-heterostructure laser [J]. *Nature*, 2002, **417**: 156-159.
[6] Hübers H -W, Pavlov S G, Semenov A D, *et al*. Terahertz quantum cascade laser as local oscillator in a heterodyne receiver [J]. *Optics Express*, 2005, **13**(15): 5890-5896.
[7] Zhou Z T, Zhou T, Zhang S Q, *et al*. Multicolor T-ray imaging using multispectral metamaterials [J]. *Advanced Science*, 2018, **5**: 1700982.
[8] Tan Z Y, Wan W J, Wang C, *et al*. Subwavelength resolved terahertz real-time imaging based on a compact and simplified system [J]. *Chinese Optics Letters*, 2022, **20**(9): 091101.
[9] Qiu F C, You G J, Tan Z Y, *et al*. A terahertz near-field nanoscopy revealing edge fringes with a fast and highly sensitive quantum-well photodetector [J]. *iScience*, 2022, **25**(7): 104637.
[10] Williams B S. Terahertz quantum-cascade lasers [J]. *Nature Photonics*, 2007, **1**: 517-525.
[11] Tan Z Y, Wang H Y, Wan W J, *et al*. Dual-beam terahertz quantum cascade laser with >1 W effective output power [J]. *Electronics Letters*, 2020, **56**(22), 1204-1206.
[12] Hosako I, Sekine N, Oda N, *et al*. A real-time terahertz imaging system consisting of terahertz quantum cascade laser and uncooled microbolometer array detector [J]. *Proceedings of SPIE*, 2011, **8023**: 80230A.
[13] Liu H C, Song C Y, SpringThorpe A J, *et al*. Terahertz quantum-well photodetector [J]. *Applied Physics Letters*, 2004, **84**(20): 4068-4070.
[14] Zhang Z Z, Fu Z L, Wang C, *et al*. Research on terahertz quantum well photodetector [J]. J. Infrared Millim. Waves.(张真真, 符张龙, 王长, 等. 太赫兹量子阱探测器研究进展[J]. **红外与毫米波学报**), 2022, **41**(1): 103~109
[15] Guo X G, Cao J C, Zhang R, *et al*. Recent Progress in Terahertz Quantum-Well Photodetector [J]. *IEEE Journal of Selected Topics in Quantum Electronics*, 2013, **19**(1): 8500508.